Check for updates

Japan Architectural Review Open Access

Architectural Institute of Japan

Original Paper

Investigation of low-disturbance seismic retrofit method for steel column bases using curved members

Kun-Sian Lin,[1] Masahiro Kurata,[2] Yutaro Kawasaki[1] and Yoshio Kitatani[3]

[1]Graduate School of Engineering, Kyoto University, Kyoto, Japan; [2]Disaster Prevention Research Institute, Kyoto University, Kyoto, Japan; [3]Daisue Construction Co., Ltd, Osaka, Japan

Correspondence
Masahiro Kurata, Disaster Prevention Research Institute, Kyoto University, Kyoto, Japan.
Email: kurata.masahiro.5c@kyoto-u.ac.jp

Funding information
JSPS KAKENHI, Grant/Award Number: 21H04574

Received August 22, 2023; Accepted December 17, 2023

doi: 10.1002/2475-8876.12429

Abstract

Seismic retrofit has always been a very important subject in recent years. However, typical retrofit techniques such as load-resisting systems, damper devices, and seismic isolation systems will cause considerable disturbances to the structural system, such as increased force demand, and the building's occupants will need to be temporarily relocated during the construction. A design of the low-disturbance retrofit method for steel column bases that uses the advantages of the curved member has been proposed in the study to improve seismic performance and reduce the mentioned demerits above. The basic mechanism of the curved member retrofit system was first analytically evaluated by preliminary modeling, followed by a parametric study to verify the effective shape. Four curved member specimens were tested with variations in fabrication processes and boundary conditions. Several aspects, including overall behavior, strength backbones, and deformation shapes of the specimens, were examined upon measured responses. The hysteretic performance of the curved member retrofit system is verified to achieve a stable cyclic behavior with limited strength degradation. A set of physical equations for estimating the lateral loads were established and verified by developing numerical models with a good agreement that enabled them to accurately represent the measured responses in the test.

Keywords
curved member, exposed column base, induction heating, low disturbance, seismic retrofit

1. Introduction

In Japan, many industrial buildings have been constructed from the late 60s to the early 90s, before the collapse of the bubble economy. These rich industrial building stocks are mostly steel structures and facing close to their life span, legally 34 years. Besides, construction material and labor prices have increased due to the international situation of the pandemic and labor shortage. Therefore, extending the lifespan of existing industrial buildings using retrofit techniques becomes increasingly important. With earthquakes such as the Great Hanshin-Awaji earthquake, the Great East Japan earthquake, and the Kumamoto earthquake, attention to the seismic resistance design for new buildings and retrofitting for existing structures is also increasing. However, seismic retrofitting techniques such as load-resisting systems, dampers, and seismic isolation systems will cause disturbances to the structure and the residents. The force demand of the structural system increases due to the increased strength and stiffness of retrofitted components. The installation and construction of seismic retrofit techniques change architectural planning and cause the temporary relocation of residents during the construction period. A study has shown a building occupancy rate of 60% during the construction period of common retrofit strategies.[1] Some recent studies focused on seismic-resilient structures that minimize both seismic damage and repair time, as well as the low disturbance to the structure were developed.[2,3]

One of the unique features of Japanese steel design is an economical design option for yielding exposed-type column bases before first-story columns, namely weak-base/strong-column design.[4] This clearly distinguishes the Japanese design from the rest of the world. The most common is pinned column bases, and column yielding is avoided by capacity design. The common approach for weak column bases is to adopt the exposed type,[5,6] consisting of a base plate welded to the column and anchor rods embedded in a concrete foundation, which is mainly used in low-rise buildings. Previous studies proposed some retrofit techniques for exposed column bases, such as using shear plates welded under the base plate to provide shear resistance,[7] and a method to eliminate the gap between the nut and the base plate by driving a wedge into the gap to convert a slip-type column base to a non-slip-type column base.[8] A commonly used retrofit method for damaged column bases by encasing reinforced concrete has been examined.[9] To retrofit damaged column bases, additional steel bars are welded to the vertical chord reinforcing steel bars embedded around the anchor rods, and reinforced concrete having such bars is formed around the steel column base. However, the behavior of the column base differs significantly by retrofit. Especially in low-rise buildings, such retrofit methods are assumed to affect the seismic demand of the frame system and existing components through changes in natural period and internal force distribution. Another study proposed a retrofit method for damaged pin-type column bases in which a constraint is used to only enhance the shear capacity of the column base.[10]

In structural design, the main reason for using curved members in building structures is often for aesthetic purposes. However, the structural efficiency, flexibility, and functionality provided by curved members such as arches and horizontally curved members also serve as attractive options for both architects and structural engineers. One of the features of curved members is the eccentricity provided by the member itself. Many studies described below have verified the benefits of the intended eccentricity provided by the component itself. For example, intended eccentricity can provide a characteristic of lateral stiffness loosely coupled with the yield strength and the ability to fulfill multiple seismic design objectives effectively in terms of stiffness, strength, and ductility.[11] An application of eccentricity in braces named crescent-shaped braces was proposed to provide enhanced seismic behavior by their geometrical configuration.[12,13] Another study proposed an A-brace design that combined pre-deformed brace segments, a steel curved damper, and a lever mechanism to amplify steel curved damper deformation for effective energy dissipation.[14] The intended initial eccentricity also controls the buckling direction, avoids the severe loss of strength due to buckling, and places the member into post-buckling behavior.[15] A novel brace that is curved and partially strengthened by induction heating was proposed, and the initial curved deformation along the brace length was proven to stabilize the compressive behavior of the brace.[16]

This study aims to propose a new retrofit method for steel column bases that combines the advantages of curved members to achieve the behavior of moderate-enhanced strength and stiffness, improved ductility, and to overcome the typical column retrofit method's weaknesses. The design and basic mechanism of the curved member retrofit system were first analytically evaluated. Four curved member specimens were tested with variations in fabrication processes and boundary conditions and applied cyclic loadings. Several aspects, including overall behavior, strength backbones, and deformation shapes of the specimens, were examined upon measured responses and test observation. The estimation equations for the strengths of the curved member retrofit system at various story drift levels were developed and compared with the measured results. A numerical model was then revised to accurately simulate experimental responses for future studies.

2. Design and Basic Mechanism

This section first proposed a retrofit technique for column bases using curved members. Numerical simulations were performed to examine the basic behavior and the design targets. Finally, the relationship between geometry and behavior such as strength, stiffness, and effective shape with a wide range of dimensions of the curved member for specimen design was verified by a parametric study.

2.1 Curved members

Although curved members are often used in buildings, their usages for the lateral load-resisting system are very few. Furthermore, the structural behavior of curved members can be much different from that of straight members. Vertically curved members in structures are subjected to combined axial compression and in-plane flexural loads, while horizontally curved members need to resist both flexural and torsional moments.[17,18] Frame systems adopting not only vertically but also horizontally curved members need to consider additional force and moment in out-of-plane directions. For vertically curved members, also known as arches, are efficient structural forms that resist loads primarily by axial compression. In practice, pure axial compression without moment cannot exist due to imperfections, eccentricities, support spreading, and unsymmetrical loading. Therefore, vertically curved members in building structures are designed for combined axial compression and in-plane flexural loads. On the other hand, horizontally curved members must resist both flexural and torsional moments. The deformed shape of a horizontally curved member is characterized by vertical and horizontal translation and torsional rotation of the cross-section. Thus, the second-order effects and the span angle of curved members are required to be considered in evaluating their strength and basic behavior.[19,20] However, previous studies and specifications mainly focused on the elastic behavior of curved members, while the research on plastic behavior is limited. In addition, curved members can be formed by many bending processes, such as cold bending and hot bending, which have different effects on their behavior and need to be investigated.

Curved channel steel has the behavior that the initial yielding region can be limited in the middle of the member under combined compression and minor axis bending, which will be described in the next section. A parametric analytical study was performed to verify the relationship between geometry and behavior, such as strength and stiffness, with a wide range of dimensions of the curved member for specimen design. A total of 11 cases of curved channel steel were considered, among which not only the height and width (H, L) but also the radius, eccentricity, and central angle (R, e, θ) of curved members were varied, as shown in Table 1 and Figure 1A. The independent parameter is the ratio of height and width, H/L, varying from 1.0 to 9.9. It should be noted that the height of the curved member is fixed at 1000 mm in the analysis. To perform the parametric analysis, a numerical model of curved members was developed using the OpenSees framework (Open System for Earthquake Engineering Simulation),[21] an open-source software framework for creating finite element applications to simulate the performance of structural and geotechnical systems subjected to earthquakes. The curved members were simulated with fiber-type force-based nonlinear beam-column elements. Ten elements were used for simulating curved segments according to the sensitivity test, which determined the robustness of the model's outcome and the recommended number of elements per AISC specification,[17,22] as shown in Figure 2. A monotonic loading was applied for all cases in the analyses to a drift ratio of 0.05 radians.

Figure 1B shows an example of the resulting analytical responses in the study. A strength backbone curve of the curved member that provides a behavior with two plastic strength capacities was first obtained for each case, as illustrated in the figure. The analytical strengths and stiffness were then obtained based on the tri-linear curve formed by the tangents of the strength backbone, as shown in Figure 1B. Based on the analytical results, the tangents of the strength backbones would gradually change after the first plastic strength since the yielding of the cross-section was gradually grown from the outer surface toward the center. Figure 3 shows the resulting analytical responses of initial stiffness and yielding strength from the parametric study. Both initial stiffness and yielding strength gradually increase in the range of the ratio of *H/L* from 1.0 to 2.5 due to the reduction in eccentricity and decrease significantly with the ratio of *H/L* >3.0 due to the change of the moment distribution. The ratio of *H/L* in the range from 1.0 to 3.0 has expected behavior and moment distribution and is therefore set as the design target range, while the moment distribution with the ratio of *H/L* >3.0 gradually changes to double-curvature-liked behavior.

2.2 Strength estimation of curved members

For the strength estimation, the curved member provides a behavior with two plastic strength capacities. The overall strengths varied with the bending processes and boundary conditions. The strengths under different drift angles were evaluated through the stress distribution over the middle and end sections of the curved member, as illustrated in Figure 4. The various axial strengths (F_{yi} and F_u) of the curved members were related to the developed axial stress and bending stress of the cross-section following Equations (1) and (2).

$$F_{yi} = \frac{\sigma_y A}{1 + (eA/S_i)} \tag{1}$$

$$F_u = \frac{\sigma_u A}{1 + (eA/Z)} \tag{2}$$

where i denotes the two yielding stages of the curved member, for example, first yielding (F_{y1}), second yield (F_{y2}). The σ_y and σ_u are the yield strength and the ultimate strength of the steel material, respectively. A is the cross-sectional area, S_i is the section modulus of the cross-section, which can be calculated by the moment of inertia divided by different distances away from the neutral axis, Z is the plastic section modulus of the cross-section, and e is the eccentricity of the curved member.

Two stages of yielding strengths and one stage of ultimate strength were considered, as shown in Figure 4. (1) The F_{y1} denotes the axial force of the curved member as the flanges at the middle of the curved channel steel reach their yield strength (σ_y). (2) The F_{y2} denotes the axial force of the curved member as the end section of the channel steel reaches its yield strength (σ_y). (3) The F_u denotes the axial force as the middle and end sections are fully yielded. The lateral strengths (Q_{yi} and Q_u) at the loading point were related to the geometry of the curved member and can be calculated by Equations (3) and (4).

$$Q_{yi} = F_{yi} \times \cos\left(\tan^{-1} H/L\right) \tag{3}$$

$$Q_u = F_u \times \cos\left(\tan^{-1} H/L\right) \tag{4}$$

where H and L are the height and the width of the curved member, respectively. It should be noted that the story drift of the strength Q_{y2} is two times greater than the story drift of the strength Q_{y1}, according to the analytical results by ABAQUS. Figure 5A presents the accuracy of the calculated results of the lateral strength with respect to the analytical results. It is shown that Equations (3) and (4) provide a good agreement between the analytical and calculated results with errors within ±15%. The error between the analytical and calculated result gradually increases with the ratio H/L >3.0 due to the changes in the moment distribution on the curved member, as shown in Figure 5B.

TABLE 1 The major parameters of samples in the parametric study

Cases	*H* (mm)	*L* (mm)	*R* (mm)	*e* (mm)	*θ* (°)
Case 1	1000	1000.0	1000	285.7	90.0
Case 2	1000	729.8	1050	196.9	72.2
Case 3	1000	641.7	1100	170.5	65.4
Case 4	1000	536.7	1200	1395	56.4
Case 5	1000	469.3	1300	120.9	50.3
Case 6	1000	420.2	1400	107.5	45.6
Case 7	1000	381.9	1500	98.7	42.8
Case 8	1000	325.2	1700	82.0	360
Case 9	1000	267.9	2000	67.3	30.3
Case 10	1000	171.5	3000	43.0	19.5
Case 11	1000	101.2	5000	25.0	11.5

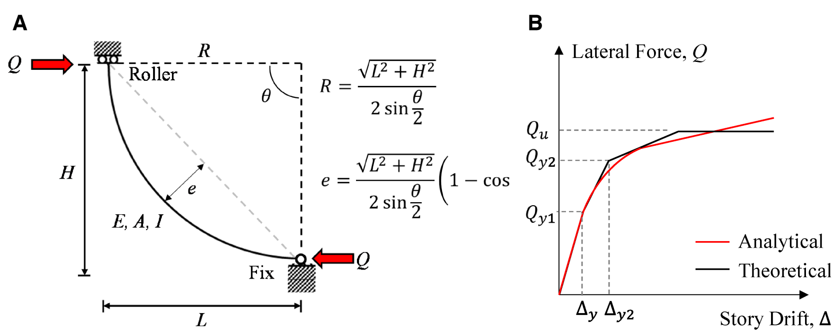

FIGURE 1 (A) Geometric parameters of the curved member and (B) illustration of the method of obtaining stiffness and plastic strength capacities upon analytical results

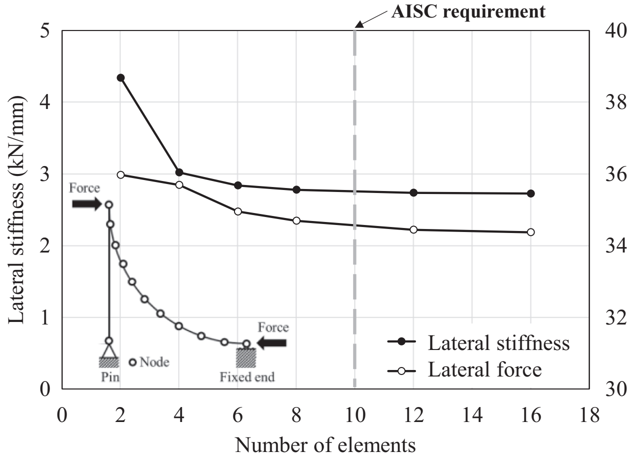

FIGURE 2 Results of sensitivity analysis

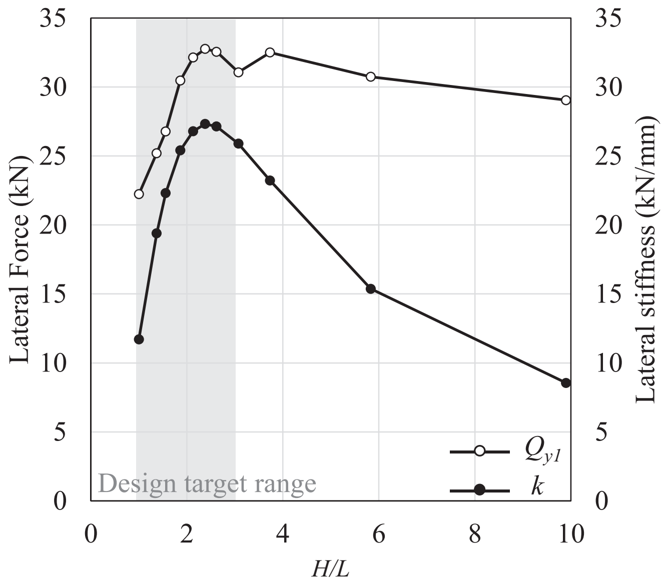

FIGURE 3 Relationship between the difference in geometry and the yield strength and lateral stiffness

2.3 Proposed retrofit technique

As shown in Figure 6, the proposed curved member retrofit system consists of two channels curved by an induction-heating process and lean against an existing column. Two curved members are connected by high-strength bolts and steel plates. The end plates welded to the channels are tied with anchor rods on the foundation and covered by a new concrete slab. The gap between the bottom ends of curved members and the concrete slab is filled with the debonding material to ensure that the performance of curved members is not affected.

The design concept is to benefit from the characteristic of curved members to achieve the behavior with a controllable yielding region. Moreover, the eccentricity provided by the curved member has the feature that lateral stiffness is loosely coupled to the yield strength. This feature enables the strength-stiffness relationship of the retrofit system to be controlled by geometric parameters and to avoid severe loss of strength by buckling. Design targets for the retrofitted column base are (a) moderate-enhanced strength, stiffness, and improved ductility; (b) enlarged plastic rotation capacity to reduce the seismic demand for the column base; and (c) minimal disturbance to the structure during and after adopting this retrofit method, as illustrated in Figure 7.

2.4 Preliminary modeling

To first examine the mechanism, performance, and design targets of the proposed curved member retrofit method, a series of pre-analyses were conducted. Numerical models of original column bases, pin-supported column bases with curved members to verify the contribution and behavior of curved members only, and retrofitted column bases representing the actual construction were developed using the OpenSees framework and ABAQUS, a software application used for modeling and analyzing mechanical components and visualizing the results.[23]

The model of the exposed column base in OpenSees was composed of a base plate and anchor rods,[24] as illustrated in Figure 8A. The base plate was modeled with a fiber section assigned to nonlinear elements outside the column depth and elastic elements with 10 times the elastic modulus inside the column depth. The anchor rod was modeled with a circular fiber section assigned to a force-based nonlinear element. The material property of anchor rods was hysteretic material in series with the rigid elastic no-compression material to simulate the slip behavior of column bases. The concrete foundation was simulated using truss elements with the material

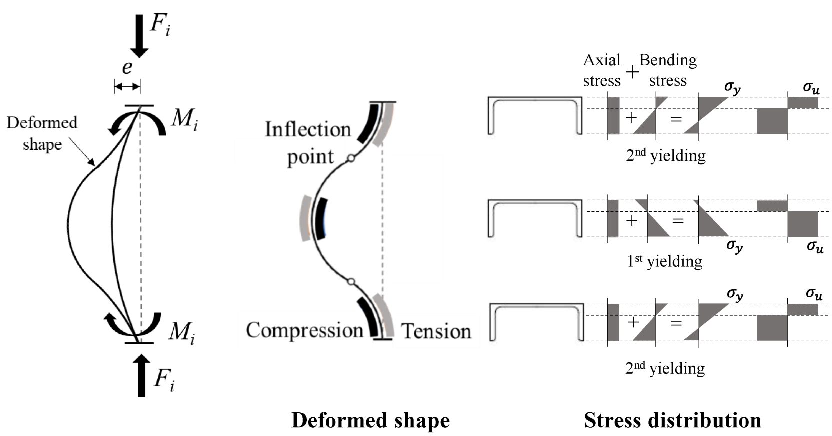

FIGURE 4 The stress distributions over the middle and end sections at various stages

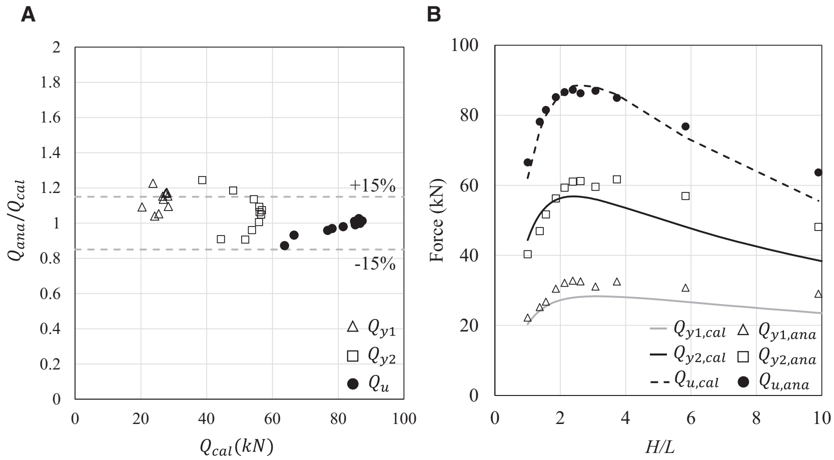

FIGURE 5 (A) Comparisons and (B) error distribution of calculated and analytical values of strength

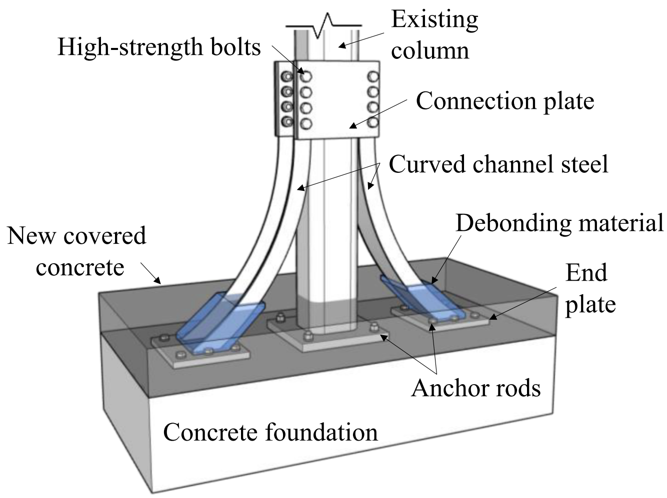

FIGURE 6 Schematic of the proposed curved member retrofit system

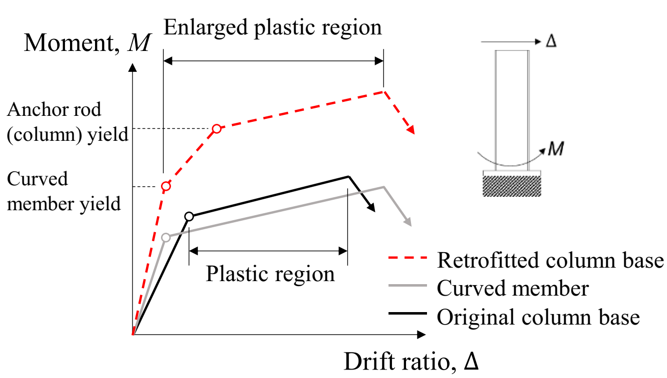

FIGURE 7 Comparison of the strength backbones of the original and retrofitted column bases

property of Concrete01, so-called Winkler springs. These truss elements were equally spaced along the base plate length. The curved channel steels were simulated with fiber-type force-based nonlinear beam-column elements as mentioned in Section 2.1.

The column base model in ABAQUS was composed of a base plate that was tied to a column. The tie constraint was used to simulate the complete joint penetration (CJP) welding at the curved member-to-end plate connection and column-to-base plate connection, as illustrated in Figure 8B. Anchor rods and mortar used surface-to-surface contact to model contact interactions between surfaces in the model. Eight-node solid elements with reduced integration are used for meshing all assemblies. To define the tangential interactions of the surface-to-surface contacts, the penalty method is used. The friction coefficients of 0.2 and 0.7 are used for steel-to-steel and steel-to-concrete interactions. Hard contact is assumed for the normal behavior of the contact surface.

2.5 Prototype design process

In this study, an exposed column base, EJ250-4-30, was adopted in the pre-analysis. The adopted column base consisted of a HSS $250 \times 250 \times 16$ column (BCR295) welded to a $410 \times 410 \times 40$ base plate (SN490B), and the base plate was tied with four rods (30 mm nominal diameter) on a grout layer. Both the OpenSees and ABAQUS models of column base EJ250-4-30 were validated with the column base component test and presented good agreement with test results in terms of strength and stiffness, as shown in Figure 9.[25]

For the adopted column base, a prototype system was designed by following steps: (1) design the curved member depth close to the adopted column depth; (2) determine the height H and width L of the curved member within the range of ratio H/L as shown in Figure 3 and architectural requirements for minimizing the disturbance to structures.; (3) determine the material and section properties of σ_y, A, and S of the curved member by Equation (3) to estimate the stiffness and strength of the retrofitted column base by the superposition principle; (4) design connections, including connection plates and end plates, of the curved member according to the capacity design philosophy; (5) check the design targets of required stiffness and strength and the moment reduction of 30% for the retrofitted column base; (6) adjust the design parameters of the curved member in steps 2 and 3 to meet the design targets. It should be noted that the numerical simulation is needed to check the behavior of curved members in step 5. In this paper, curved channel steel with section $200 \times 80 \times 7.5 \times 11$ with a height of 1000 mm and a width of 470 mm was adopted for the prototype retrofit system and examined in Section 2.6.

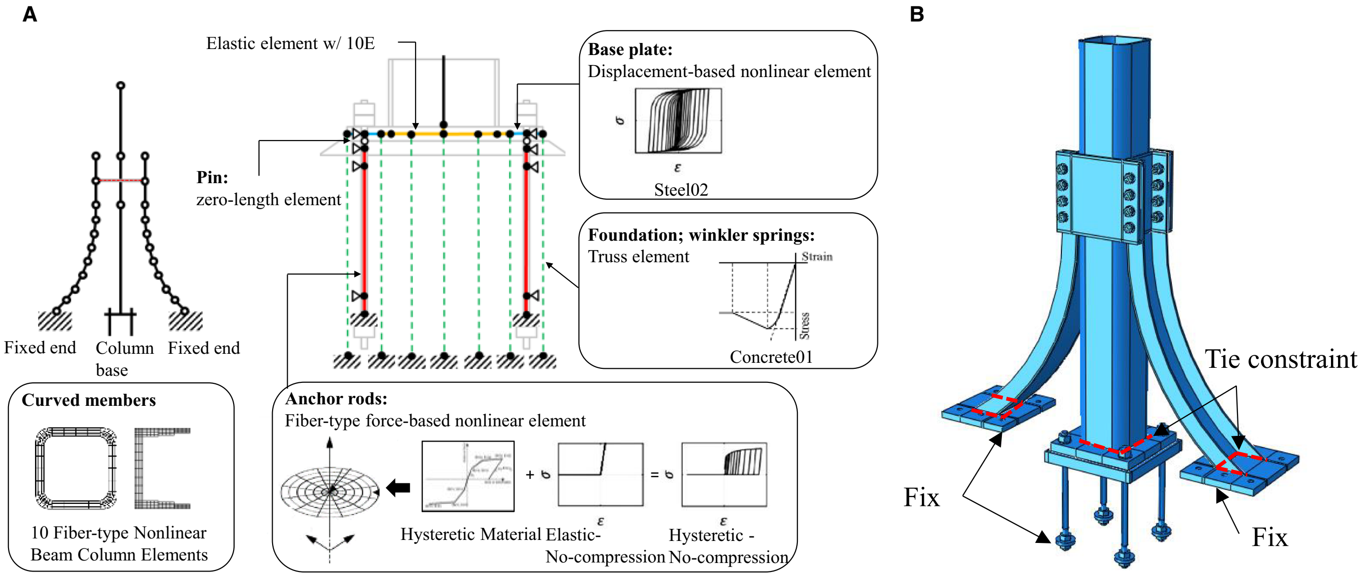

FIGURE 8 Illustrations of the adopted column base model in (A) OpenSees and (B) ABAQUS

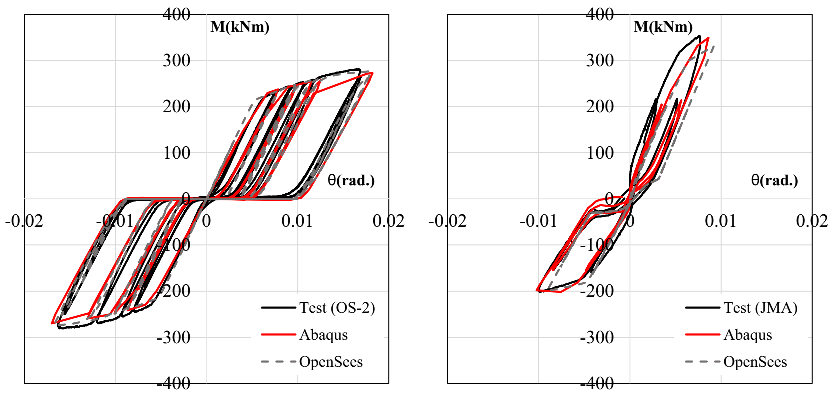

FIGURE 9 Comparisons of measured and analytical hysteretic responses in column bases

2.6 Basic behavior and check of design targets

The design target for the retrofitted column base mentioned above includes having the behavior of moderate-enhanced strength, stiffness, improved ductility, and enlarged plastic rotation capacity to reduce the seismic demand for the existing column base. Moderate-enhanced strength and stiffness can be achieved by controlling the geometric parameters of curved members, such as eccentricity and height. Improved ductility is achieved by the enlarged plastic region, with plastic strength corresponding to the early yielding of the curved member and the delayed yielding of the anchor rods at the original column base. Figure 10 shows the analytical results, including the behavior of the original column base, the curved member retrofit system with a mechanic pin at the bottom of the column, and the retrofitted column base from ABAQUS. The analytical results of the retrofitted column base show that the first yielding started at the middle of the curved member at the drift angle of 0.01 radian, followed by the yielding at the ends of the curved member at the drift angle of 0.016 radian, indicating the early yielding mechanism can be achieved and controlled at the middle of the curved member. The anchor rods started yielding at the drift angle of 0.014 radian for the original column base, while the yielding was delayed to the drift angle of 0.019 for the retrofitted column base by the curved members with reduced moment demand. The drift angle of anchor rods yielding at the retrofitted column base has been increased by 36% compared with the original column base. It indicates that the proposed retrofit system enables to enlarge the plastic rotation capacity of the original column base and reduces its seismic demand.

For comparison, the analysis that only focused on the behavior of curved and straight members adopted in the proposed retrofit system was performed, indicating a significant difference. The design concept of the proposed retrofit method is to use the advantages of curved members. However, we need to verify the reasons for adopting the curved member instead of its straight counterpart. The behavior of the retrofit system adopting straight members had larger initial stiffness and yield strength with the early occurrence of local buckling, which resulted in strength degradation, while the one adopting curved members had controllable initial stiffness and yielding strength with great ductility, as shown in Figure 11.

The proposed retrofit method aims to moderately increase the initial stiffness, strength, and ductility capacity of the original column base to meet the required capacity but doesn't significantly change the natural period of the structure, which results in increased seismic demand. Therefore, the design target of minimal disturbance to the structure during and after adopting this retrofit method, such as (a) weld-free on the column and easy construction; (b) small amount of space occupancy; and (c) minimizing the increased seismic demand of the frame system, was analytically verified by adopting this retrofit method on a four-story SMRF that was designed for a hospital facility. The structural design followed the building law of Japan, with a reserved strength of 1.5 times to the code minimum. The general floor plans and elevations of the four-story building were designed as 2 by 1 bays of 5.0 and 7.0 m, respectively, with a story height of 3.6 m for the first story and 3.4 m for the rest of the stories, as shown in Figure 12A. The member sizes of beams and columns in the SMRF building are given in Table 2, and the exposed column bases adopted were EJ250-4-30. The frame system was developed using the OpenSees framework and validated with data from the E-defense shaking table test[25] by dynamic analysis. All beams and columns were simulated using force-based nonlinear beam-column elements combined with fiber-type sections with five integration points for each element. The effect of the panel zone was considered in the model using the method as a rectangle composed of eight very stiff elastic beam-column elements with one zero-length element that serves as a rotational spring to represent shear distortions. The P-delta effect of the frame was included, and the floor weights were distributed on the beams at each floor level of the models. The nodes at each floor level were mastered by the very middle node of the floor in the degree of freedom of horizontal displacement to simulate the rigidity of the slabs. The uniaxial material model of Steel02 was calculated using the yield strength and the kinematic strain hardening ratio determined by the material tests for each fiber.

The adopted retrofit system used curved channel steels ($200 \times 80 \times 7.5 \times 11$) and was determined to have a height and width of 1300 and 800 mm, respectively, to match the dimension of the columns, and was covered by a 200 mm thickness of concrete. The resulting space occupancy rate for the building that adopted the retrofit system is 16% in a single span on the first floor compared to the original building. To verify the influence on the frame system, the static pushover analysis that used the equivalent lateral force (ELF) recommended by FEMA 273 was performed for the four-story SMRF and the same building adopting the curved member retrofit system (SMRF-CM). The analytical results show that the natural

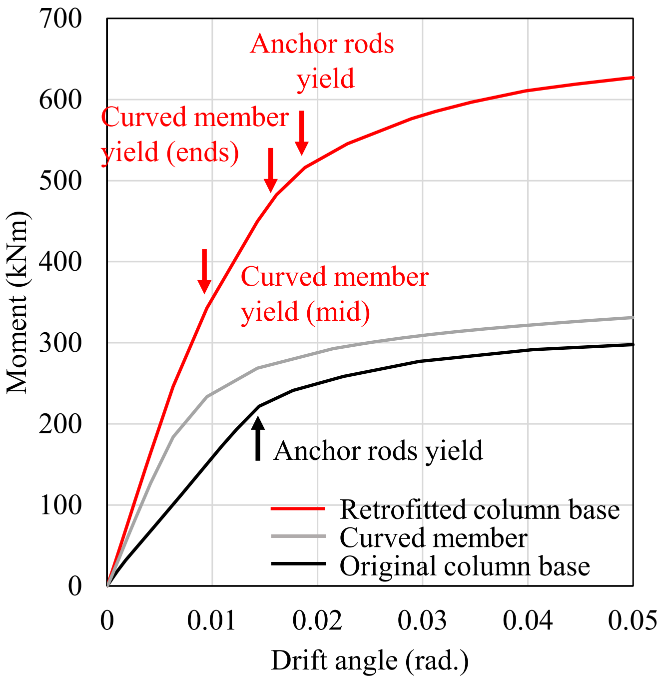

FIGURE 10 Comparison of analytical responses of curved members, original, and retrofitted column bases

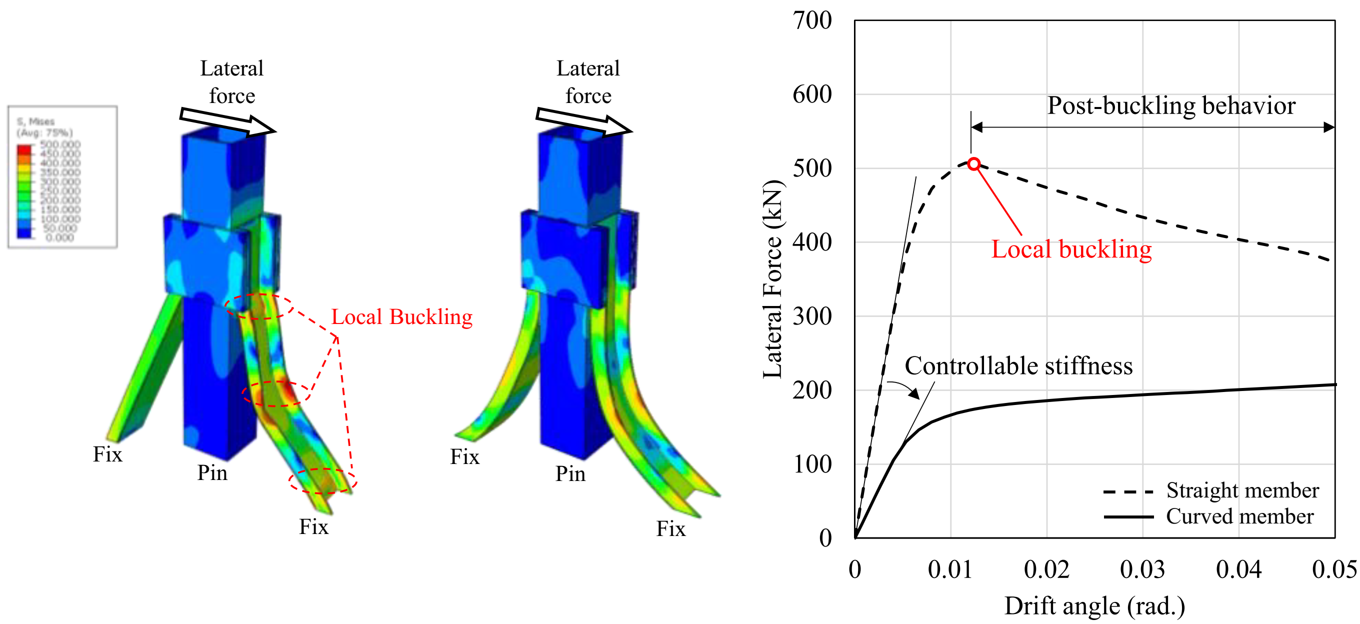

FIGURE 11 Comparison of analytical responses for the retrofit system using straight and curved members

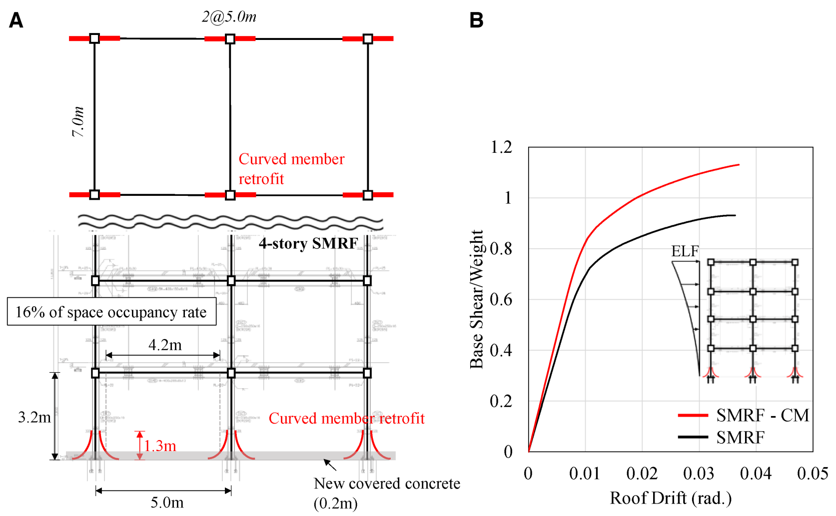

FIGURE 12 (A) Plans and elevations and (B) pushover curve of the adopted four-story SMRF with curved member retrofit system

TABLE 2 Designed member sizes of the four-story buildings

Prototype buildings	Stories	Beams (mm)	Columns (mm)
SMRF4F	1	H-400 × 200 × 8 × 13	□-250 × 250 × 16
	2	BH-400 × 150 × 6 × 19	□-250 × 250 × 16
	3–4	H-400 × 200 × 8 × 13	□-250 × 250 × 16

period of the four-story SMRF with curved member retrofit has a 6% reduction, and the stiffness and strength are increased by about 19% compared to the original structure, as shown in Figure 12B. It implies that the proposed retrofit system won't increase much seismic demand on the overall frame system.

Figure 13 shows the moment distributions on the first-floor column of the four-story frame systems (SMRF-CM and SMRF) for comparing the difference between the retrofitted and the original column bases under various lateral force levels. The analytical results show that the moments at the column base and the beam connection of the retrofitted column base are smaller than those in the frame without the retrofit. It is indicated that this retrofit method is not only effective in the frame subjected to horizontal forces but also reduces the demand on the original column base.

3. Test Program and Test Setup

An experimental program has been conducted to examine the proposed curved member retrofit system, focusing on the behavior of curved members and evaluating their influence on different boundary conditions and fabrication processes. Four cases of a curved member retrofit system have been tested by applying lateral cyclic loadings.

3.1 Overview loading setup

The lateral cyclic loadings were applied by two 1500 kN actuators through a relatively stiff apparatus at the top. The apparatus was connected to the column (HSS 250 × 250 × 12) at the top, while the lower end was connected to a mechanic pin, representing a simple column base. Two identical specimens lean against the column and are connected by high-strength bolts and steel plates. The end plates welded to the specimens were tied with high-strength bolts to the fixture in the test. It should be noted that by adjusting the axial force of two actuators, no axial force was applied to the column in tests. Figure 14 shows the adopted test setup in the study with a photo of an installed specimen.

3.2 Specimens

All curved member specimens in the study had the same dimensions (Channel 200 × 80 × 7.5 × 11), including 936 and 350 mm in height of the curved segment and connection segment, respectively, and 1200 mm in radius. At the intersection between the channel steel and the end plate, the complete joint penetration (CJP) welds were used. The detailed dimensions of the specimen are shown in Figure 15. A steel grade of JIS-SS400 was adopted for each specimen in the study. Table 3 presents the measured material properties of the adopted channel steel based on the tensile tests per the ASTM E8/E8M-13a (2013) standard. Four types of coupon specimens, including standard specimens, heat-treated specimens, induction-heating bending specimens, and cold-form bending specimens, were tested to examine the effects of different fabrication processes. The coupon specimens were made from the flange and web of channel steels; therefore, the coupon specimen made from the web has the same curvature as the channel steels, as shown in Figure 16A. It should be noted that the stress–strain curve output from strain gauges for coupon specimens with initial curvature has a straightening process at the beginning of the test, as shown in Figure 16B.

The differences between specimens were the fabrication process and the boundary conditions. Fabrication processes for curved members can be divided into cold bending and hot bending. Cold bending is a method of processing mainly at room temperature to 720°C with the feature of densifying the metallographic structure of steel, which is usually more economical than hot bending or induction-heating bending. In addition, the metal is not subjected to excessive temperature by cold bending, while the residual stress is generated inside and the yielding stress increases due to strain hardening. The effect of residual stress on structural performance has been proven to not affect the plastic strength of the member, while both the local and global buckling strength of compression members can be affected depending on external circumstances.[17,26,27] The cold bending process also needs to apply a large force, and processing accuracy needs to consider the material springback. The common cold bending process is known as roll bending, in which members are bent using rollers, and was adopted for the cold-form bending specimens in the test. Induction-heating (IH) bending is an advanced hot bending process that utilizes an electric induction coil to heat a narrow band around the member circumference before it is bent by force, offering great precision and consistency. IH bending is suitable for a wide range of applications and overcomes the potential limitations of cold bending, such as

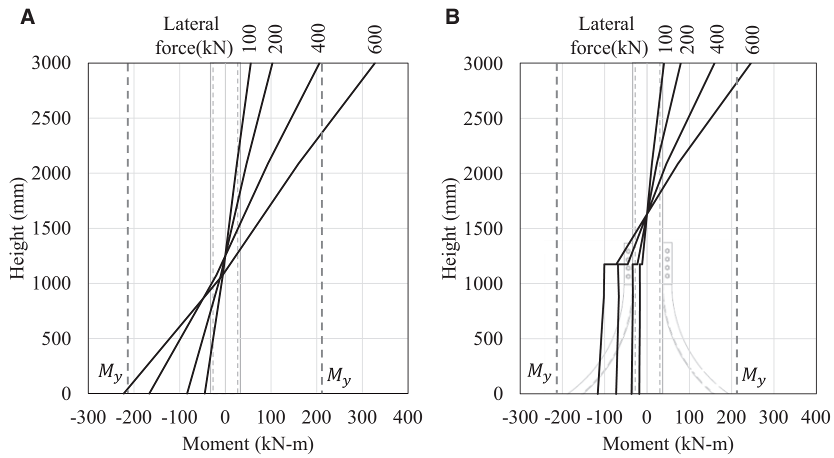

FIGURE 13 Moment distribution of the column in the frame system with (A) original column bases and (B) retrofitted column bases

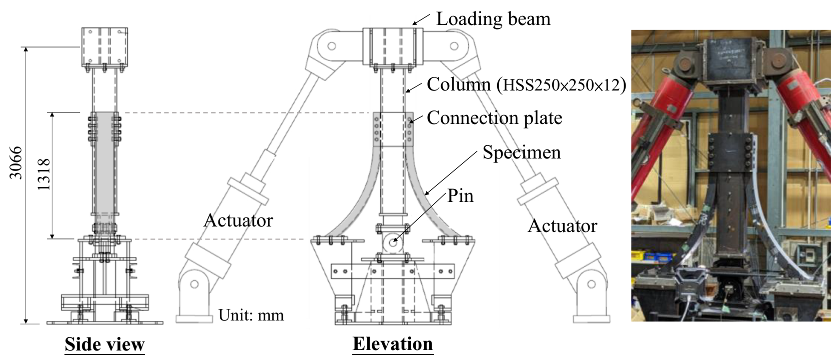

FIGURE 14 Elevations and a photo of adopted test setup in the experimental program

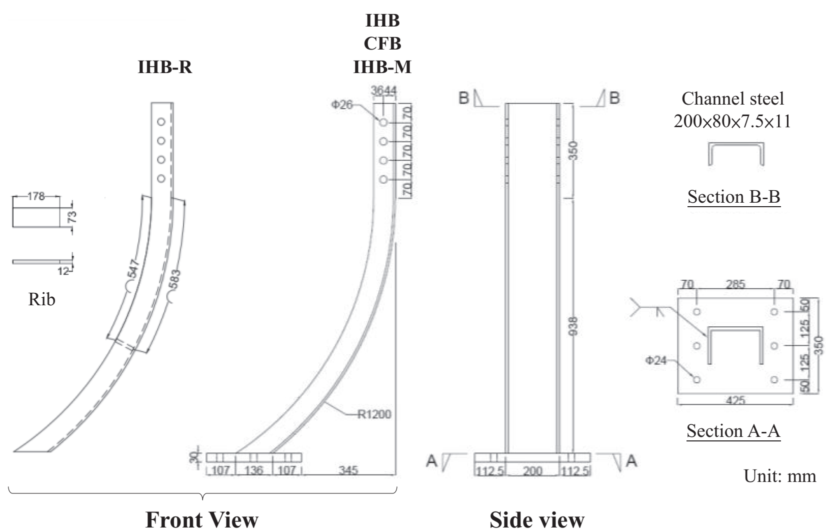

FIGURE 15 Detailed dimensions of specimens in the study

distortion, wall thinning, and residual stress. The IH bending for the specimens in the test is processed by applying heat at 750°C and then air cooling to room temperature.

Four specimens for the curved member retrofit system have been tested. IHB presented a baseline specimen bent using induction heating, while IHB-R presented a case having the identical bending process as IHB, but with a 12-mm-thickness rib at the middle of the curved member to prevent local buckling. CFB presented a counterpart specimen bent using the cold-form process to clarify the effect of different bending processes on the behavior compared to the IH bending specimen. IHB-M presented a specimen having the identical bending process as IHB, but with a 50 mm thickness mortar below the end plate to simulate the actual construction. It should be noted that there was no pre-tension applied to the bolts connecting the end plate and the fixture to simulate the anchor rods, and the shear force was resisted by the friction between the end plate and the mortar. The connecting rods, which connect two end plates, were used to transmit the force resisted by friction in cyclic loading.

3.3 Loading protocol

A cyclic loading protocol with increasing amplitudes from a lateral drift angle of 0.375%–5.0% radians was adopted, as shown in Figure 17A. In addition, one extreme cycle of 10.0% drift angle was performed following the standard loading protocol to examine the failure mode of the specimens.

Figure 17B shows the measuring instruments used in the test, including strain gauges to output the moment on the curved member specimen and a load cell in the mechanic pin to measure the lateral and vertical force on the column. Two LVDT sensors were used to measure the relative displacement of the end plates and the fixture. The camera system was adopted to measure the overall and out-of-plane deformation of the specimen.

TABLE 3 Material properties upon coupon test

Fabrication process	Steel grade	Nominal plate thickness (mm)	Nominal elastic modulus E (GPa)	Measured yield strength F_y (MPa)	Measured tensile strength F_u (MPa)
Standard	SS400	7.5	200	312.0	429.0
Induction-heating w/o bending				323.0	437.2
Induction-heating bending				318.9	437.0
Cold-form bending				358.4	489.9

4. Measured Responses and Test Observation

Four specimens were tested with variations in the fabrication process and boundary conditions and applied cyclic loadings. Several aspects, including overall behavior, strength backbones, and deformation shapes of the specimens, were examined upon measured responses and test observation. In addition, the developed numerical model was validated with test results.

4.1 Overall behavior

The measured hysteretic responses of all cases are shown in Figure 18. All cases provided stable cyclic behavior with very limited strength degradation by the end of the applied cyclic loading. Various lateral load capacities were shown among cases due to the differences in the bending processes and the boundary conditions.

Upon the test observations, the curved member specimens started yielding on the flange at the middle of the curved member at the drift angle of 1.0% radians, and the end section of the curved member started yielding at the drift angle of 2.0% radians. Several behaviors were observed in the tests, including local buckling (LB), slipping at the bolt connection at the top of the specimen, and the end-plate slipping, as shown in Figure 19. It should be noted that the fixture below the specimen was observed to move during the tests of IHB and IHB-R and resulted in an asymmetric initial elastic stiffness of the specimens. Figure 18A shows the measured hysteretic responses of the specimen IHB. The IHB developed the yielding in the cycles of 1.0% drift angles. It should be noted that due to the movement of the fixture observed in the test, the local buckling of IHB actually occurred in the cycles of 4.0% drift angles instead of 5.0% drift angles, as shown in Figure 18A. Slipping of the bolted connection at the top of the specimen was observed in the cycles of 3.0% drift angles and resulted in some pinching behavior under large deformation. The measured responses of the specimen with ribs (IHB-R) at the middle of the curved member are shown in Figure 18B. After eliminating the effect of fixture movement, the local buckling of IHB-R occurred earlier in the cycles of 3.0% drift angles compared to the IHB. Upon the test observations, it was shown that the specimen IHB had more distributed yielding on the flange around the middle of the curved member compared to IHB-R, where the yielding area was only concentrated on the flange above the ribs before the cycles of 4.0%

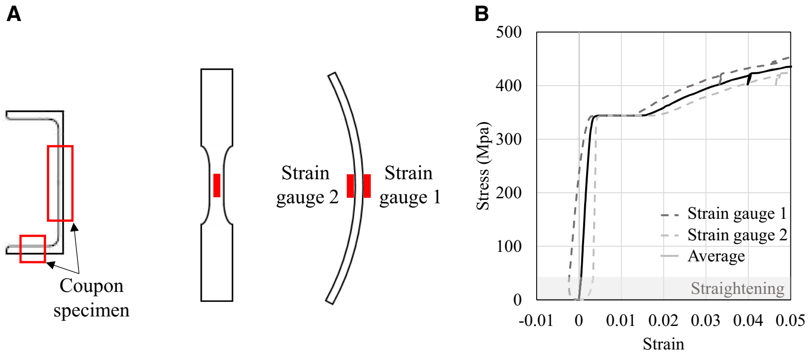

FIGURE 16 (A) locations of the coupon specimen from channel steel and (B) the stress–strain curve of the specimen with curvature

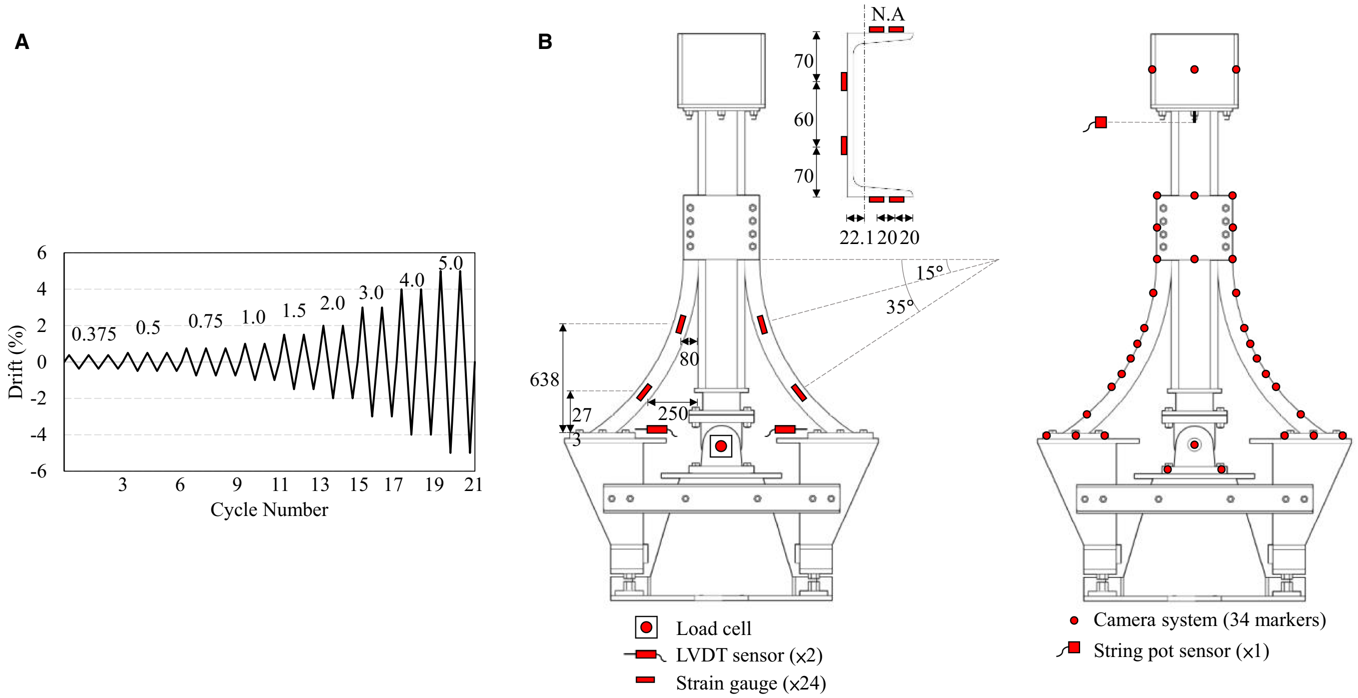

FIGURE 17 (A) Adopted cyclic loading protocol and (B) adopted measuring instruments

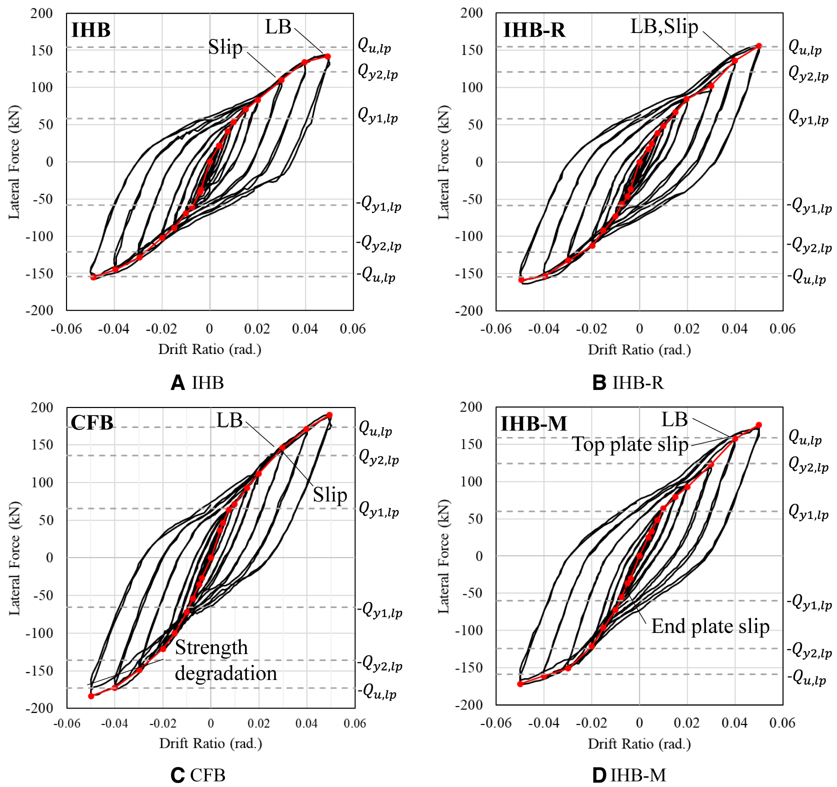

FIGURE 18 Measured hysteretic responses. (A) IHB. (B) IHB-R. (C) CFB. (D) IHB-M

drift angles, as shown in Figure 18. It is shown that IHB-R developed slightly higher strength than the IHB. The effect was considered to be related to the level of strain concentration, which increased the strain demand at the middle of the curve member specimen and thereby developed more strain hardening as well as the lateral strengths. It also implied that the rib would, however, advance the deformation concentration around the rib of the specimen and have limited improvement in preventing local buckling. The rib arrangement was not effective here. For evaluating the effect of the cold-formed

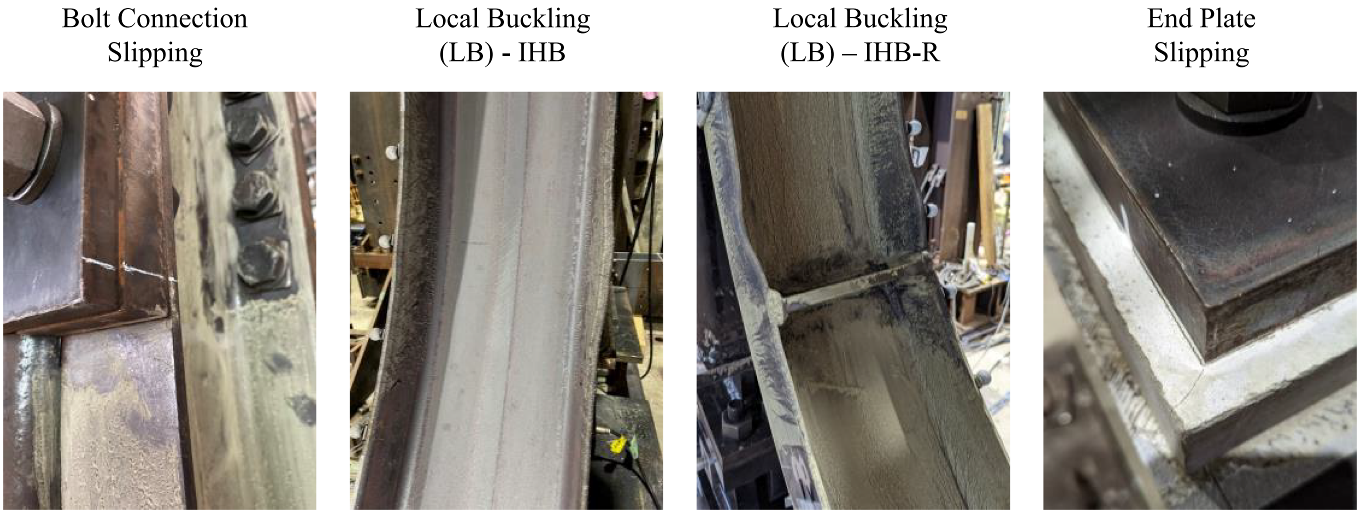

FIGURE 19 Photos of the observed behaviors of the specimens

bending process on the behavior, specimen CFB, which had identical dimensions to the IHB, was tested. Figure 18C shows the measured responses of CFB. The local buckling occurred in the cycles of 3.0% drift angle, and strength degradation was observed in the second cycle of 5.0% drift angle. CFB developed 1.15 times the lateral strength of IHB, corresponding to the coupon test, due to the strain hardening effect caused by the cold-formed bending process, corresponding to the results of the material test. In addition, the initial distortion and poor precision of the specimen CFB caused by the cold-form bending resulted in difficult installation in the test. It should be noted that the locations and shapes of local buckling of CFB were observed corresponding to the initial distortion of the specimen. The measured responses of the specimen with mortar (IHB-M) below the end plate are shown in Figure 18D. It is shown that IHB-M had higher strength than the IHB due to the thickness of the mortar and that the specimen is relatively close to the loading point. The end-plate slipping of IHB-M occurred in the cycles of 0.5% story drift but had no influence on the behavior such as severe strength degradation and pinching. The local buckling occurred in the cycles of 4.0% drift angle, as shown; no strength degradation was observed throughout the loading protocol, implying its feasibility in practical applications.

The lateral strengths at the loading point ($Q_{yi,lp}$ and $Q_{u,lp}$) of the retrofit system were related to the dimensions of the existing column and the geometry of the curved member specimens. Equations (3) and (4) established in Section 2 could be used to develop the estimation equations for the actual strength backbones at the loading point of the retrofit system following Equations (5) and (6).

$$Q_{yi,lp}=\left[2F_{yi}\cos\left(\tan^{-1}\frac{H}{L}\right)H_p+F_{yi}\sin\left(\tan^{-1}\frac{H}{L}\right)d_c+2F_{yi}e\right]/H_c \tag{5}$$

$$Q_{u,lp}=\left[2F_{u}\cos\left(\tan^{-1}\frac{H}{L}\right)H_p+F_{u}\sin\left(\tan^{-1}\frac{H}{L}\right)d_c+2F_{u}e\right]/H_c \tag{6}$$

where H and L are the height and the width of the curved member, respectively; H_p is the distance between the mechanic pin and the top connection of the specimen; and d_c and H_c are the depth and height of the existing column, respectively.

The resulting values of those calculated plastic strengths at the loading point of the retrofit system are marked in Figure 18 to compare with the measured responses, and it is shown that the calculated results enable them to represent the measured lateral plastic strengths of the test responses. Equations (5) and (6) were therefore verified to accurately estimate the first and second yielding and the ultimate strength of the curved member retrofit system.

4.2 Modeling validation with test results

To extend the test results to further analysis, a numerical model was developed in the OpenSees (Open System for Earthquake Engineering Simulation) framework to simulate the cyclic behavior of the curved member retrofit system. Figure 20 illustrates the proposed numerical model adopted for the curved member specimens and the fixtures in the test.

The simulation approach of the curved member mentioned in Section 2.1 was adopted in the model. The uniaxial material model of Steel02 using the yielding strength upon material test presented in Table 3 was applied to each fiber. In addition, two fiber-type force-based nonlinear beam-column elements with the section of connection plates were used to simulate the connection. The slave nodes at the side of the connection were mastered by the middle node of the column in the degree of freedom of horizontal displacement and in-plane rotation. The nodes at the end of the specimen were mastered by the nodes at the top of the fixtures to the same degree of freedom. For the fixtures below the specimens, elastic beam-column elements were adopted with exact cross-sectional dimensions used in the test to simulate the contribution to the lateral stiffness of the fixture compared to the ideal situation with fixed ends. Fiber-type displacement-based elements with the hysteretic material were adopted for channel steel, which connects the fixtures to simulate the asymmetric behavior in the first few cycles observed in the test. The mechanic pin was simulated by zero-length elements with extremely low in-plane rotational stiffness and fixed in the rest of the degrees of freedom.

The resulting analytical responses of the IHB and CFB are shown in Figure 21 compared to the measured responses. The developed numerical model generally presented high accuracy

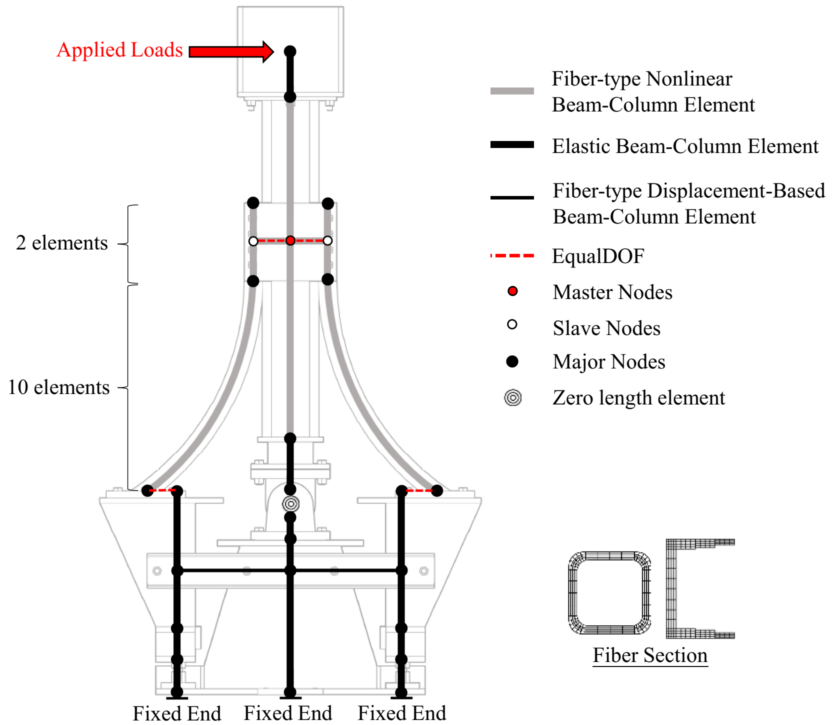

FIGURE 20 Illustration of the adopted numerical model of the specimens with the loading frame system

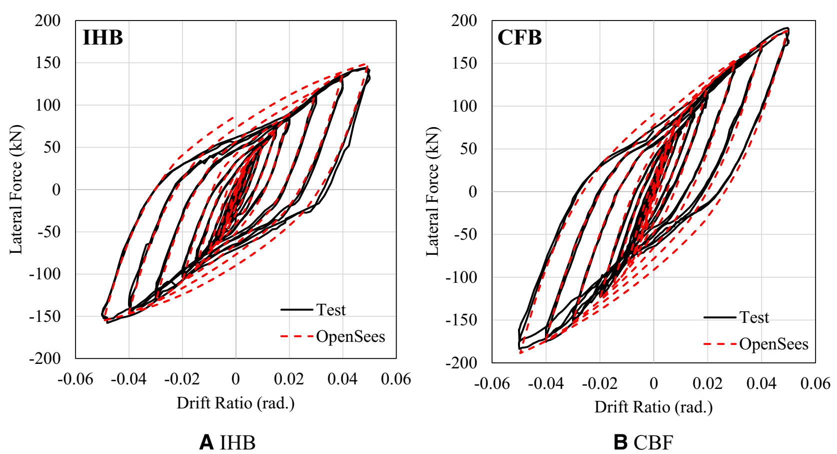

FIGURE 21 Comparisons of simulated and measured hysteretic results. (A) IHB. (B) CBF

and good agreement with the test results in terms of strength and stiffness. It should be noted that the model of fiber sections was based on the assumption of plane section remain plane and was unable to simulate the strength degradation caused by local buckling in CFB. In addition, the pinching behavior caused by the slipping at the bolt connection was not simulated in the model. The developed numerical model of the curved member retrofit system could generally be adopted for analytical study at structural system levels.

4.3 Deformed shape and deformation concentration

To evaluate the lateral displacement and the deformed shapes of the specimens, a camera system was adopted in the instrumentation of the study. The markers of the camera system were attached to the flange of each specimen, as shown in Figure 22A. The eccentricity of the specimen is one of the important parameters for estimating the strength capacity, and it will change with the deformation of the specimen. Upon the measured results, the in-plane displacements of IHB along the height of the right specimen at various drift angles are shown in Figure 22B. The results show that the in-plane displacement had an apparent change after a 4.0% drift angle. It is noted that all specimens have a similar deformed shape in the test. The ratio of eccentricity (e) to initial eccentricity (e_{initial}) of IHB, IHB-R, CFB, and IHB-M at various drift angles can be calculated from the measured responses of markers, as shown in Figure 23A–D, respectively. It should be noted that the markers on CFB fell off at the drift angle of 5.0% in the test. The results show that the eccentricities of all specimens will not exceed 1.1 times the initial value before

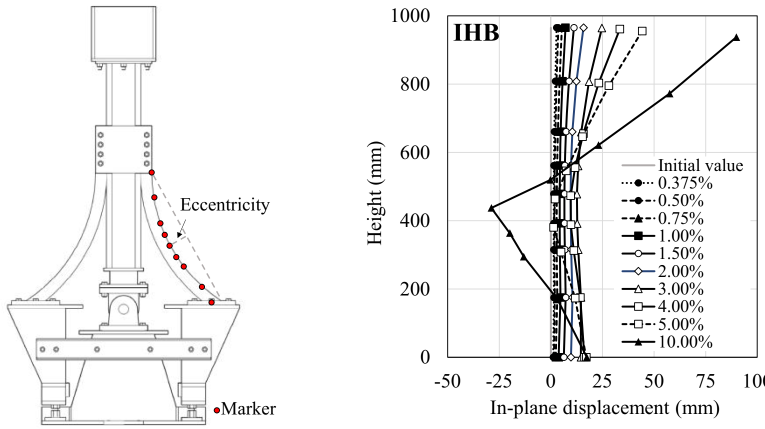

A Marker placement of camera system **B** Baseline specimen IHB

FIGURE 22 Marker placement of the camera system and deformed shape at various drift angles. (A) Marker placement of camera system. (B) Baseline specimen IHB

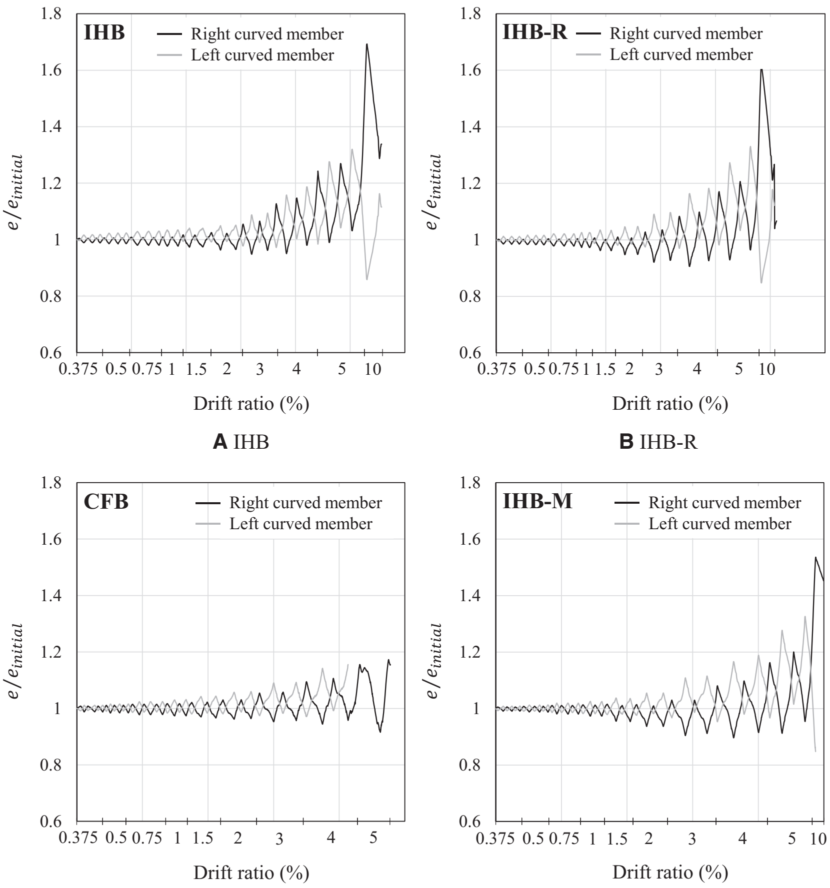

A IHB **B** IHB-R

C CFB **D** IHB-M

FIGURE 23 Measured eccentricity of each specimen at various drift angles. (A) IHB. (B) IHB-R. (C) CFB. (D) IHB-M

the 4.0% drift angle. It implied that the impact of eccentricity changes on strength capacity estimation was limited before large deformation. The initial eccentricities of both the right and left sides of IHB, IHB-R, and IHB-M were 128, 131, and 134 mm, respectively. However, the initial eccentricities of the right and left sides of CFB are 129 and 137 mm, respectively. It is considered that this effect is due to the initial distortion and poor precision of specimen CFB caused by the cold-form bending process.

The out-of-plane deformation of the specimens IHB, IHB-R, CFB, and IHB-M at various drift angles is shown in Figure 24A–D, respectively. The shadow areas in Figure 24B present the location of the rib. In Figure 24A,D, the results of IHB and IHB-M show that the flexural deformations along the

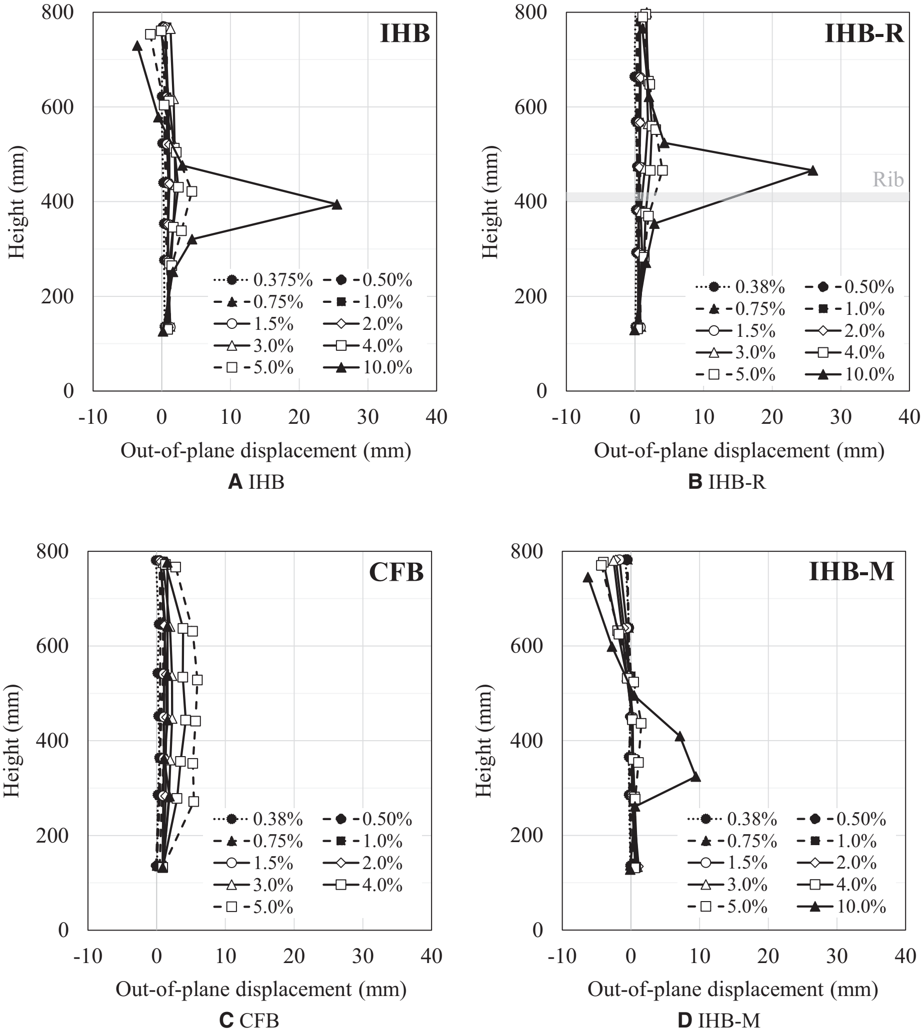

FIGURE 24 Out-of-plane displacement distributions at various drift angles. (A) IHB. (B) IHB-R. (C) CFB. (D) IHB-M

member were controlled and limited around the middle of the curved member at the member height of 420 mm. Figure 24B shows the results of IHB-R that the rib at the middle of the curved member led to greater deformation concentration at the member height of 450 mm, which would result in early local buckling in the cycles of 4.0% drift angles.

Figure 25A shows a photograph of the deformed shape of the specimen IHB under a 5.0% drift angle. It was shown that the yielding region was distributed uniformly at the middle of the curved member. The cold-formed bending specimen CFB presented a relatively uniformed out-of-plane displacement along the member height, as shown in Figure 24C. However, the test observation has shown that the local buckling occurred early in the cycles of 3.0% drift angle compared to IHB and had severe deformation concentrations under 5.0% drift angle, as shown in Figure 25B. It should be noted that the out-of-plane deformed shapes of CFB were observed, corresponding to the initial distortion of the specimen caused by the cold-formed bending process.

A IHB **B** CFB

FIGURE 25 Photographs of the deformed shapes under a 5% drift angle. (A) IHB. (B) CFB

5. Summary and Conclusions

A design of the curved member retrofit system has been proposed in the study that combines the advantages of curved members to provide the behavior of moderate-enhanced strength, stiffness, and improved ductility compared with the common retrofit method for column base. The basic behavior, performance, and design targets of the proposed retrofit system were analytically examined by pre-analysis. Four curved-member specimens have been tested, focusing on the behavior of the specimens. The effects of different fabrication processes and boundary conditions on the behavior of the specimens were investigated. Moreover, a numerical model of the curved member retrofit system was developed and validated by the experimental results. Based on the analytical and experimental work in the study, several remarks can be drawn, as follows:

1. The proposed curved member retrofit system has been analytically verified to achieve design targets including (a) moderate-enhanced strength, stiffness, and improved ductility; (b) enlarged plastic rotation capacity to reduce the seismic demand for the column base; and (c) minimal disturbance to the structure during and after adopting this retrofit method.
2. According to numerical simulations, the behavior of the proposed curved member retrofit system was verified as follows: Improved ductility of the retrofitted column base was achieved by the enlarged plastic region, with plastic strength corresponding to the early yielding of the curved member and the delayed yielding of the anchor rods at the original column base. The moments at the column base and the beam connection of the retrofitted column base are smaller than those in the frame without the retrofit. The drift angle of anchor rods yielding at the retrofitted column base has been increased by 36% compared with the original column base. It indicates that the proposed retrofit system enables to enlarge the plastic rotation capacity of the original column base and reduces its seismic demand.
3. The basic mechanism and behavior of the curved members, considering various geometric parameters and different boundary conditions, were verified. The ratio of H/L in the range from 1.0 to 3.0 has expected behavior and moment distribution and is therefore suggested as the design target range.
4. A set of theoretical equations for estimating the lateral load capacities were proposed and verified by developing numerical models with a good agreement that enabled them to accurately represent the measured responses in the test.
5. A prototype design process for the proposed curved member retrofit system based on the numerical simulation in the study was provided to achieve the design targets. Further analysis is required, and a more detailed and comprehensive design process will be developed in future research.
6. The mechanics of induction-heating and cold-formed bent curved channel steel have been experimentally verified. It is shown that induction-heating bent specimens provided a stable cyclic behavior with limited strength degradation and controllable yielding region distributed around the middle of the curved member. However, the initial distortion and poor precision of the cold-formed bending specimen in this test likely resulted in early local buckling, strength degradation, and difficult installation. It should be noted that the fabrication accuracy depends on the fabricator, and the cold-formed bending member can also be adopted in the proposed retrofit system if fabrication accuracy is met.
7. The end-plate slipping of IHB-M occurred in the cycles of 0.5% story drift but had no influence on the behavior such as severe strength degradation and pinching. The local buckling occurred in the cycles of 4.0% drift angle; no strength degradation was observed throughout the loading protocol, implying its feasibility in practical applications.

Acknowledgments

The technical advises from the JSSC Kansai regional committee on the Use of Information Technology in the Construction and Fabrication of Steel Members and Hokuriku Kenko are appreciated. This research was under the collaborative research of Kyoto University and Daisue Construction Co., Ltd and was partially supported by JSPS KAKENHI 21H04574.

Disclosure

The authors have no conflict of interest to declare.

Data Availability Statement

The data that support the findings of this study are available from the corresponding author upon reasonable request.

References

1. Takeuchi T, Yasuda K, Yuasa K, Okayama S, Miyazaki K, Iwata M. Seismic retrofit of aged building with integrated facade. *AIJ J Technol Des*. 2006;**12**(24):161-166.
2. Lavan O, Sato M, Kurata M, Lei Z. Local deformation-based design of minimal-disturbance arm damper for retrofitting steel moment-resisting frames. *Earthq Eng Struct Dyn*. 2017;**46**(9):1493-1509.
3. Kurata M, Sato M, Zhang L, Becker T, Lavan O, Nakashima M. Seismic retrofit of steel frames with minimal-disturbance. In *IABSE Conference: Elegance in Structures*, Nara, Japan; 2015:398-399.
4. Akiyama H. *Seismic Design for Steel Column Base*. Giho-Do Press; 1985 (in Japanese).
5. Hassan AS, Song B, Galasso C, Kanvinde A. Seismic performance of exposed column–base plate connections with ductile anchor rods. *J Struct Eng*. 2022;**148**(5):04022028.
6. Hassan AS, Torres-Rodas P, Giulietti L, Kanvinde A. Strength characterization of exposed column base plates subjected to axial force and biaxial bending. *Eng Struct*. 2021;**237**:112165.
7. Udagawa K, Kusaka A, Saeki T, Fukuta T, Morita K. Effects of postearthquake modifications of exposed steel column bases. *Steel Constr Eng*. 1997;**4**(15):1-13.
8. Takamatsu T, Tamai H. Non-slip-type restoring force characteristics of an exposed-type column base. *J Constr Steel Res*. 2005;**61**(7):942-961.
9. Nakashima S. Mechanical characteristics of steel column-base connections repaired by concrete encasement. In *Proceedings of the Tenth World Conference on Earthquake Engineering*, Madrid, Spain; 1992:5131-5136.
10. Yamada S, Shimada Y, Ishida T, Sawada R. Transferring method of shear force in pin-type column base for seismic retrofit. *J Struct Constr Eng Trans AIJ*. 2014;**79**(695):145-152.
11. Trombetti T, Silvestri S, Gasparini G, Ricci I. Stiffness-strength-ductility-design approaches for crescent shaped braces. *Open Constr Build Technol J*. 2009;**3**(1):127-140.
12. Palermo M, Pieraccini L, Dib A, Silvestri S, Trombetti T. Experimental tests on crescent shaped braces hysteretic devices. *Eng Struct*. 2017;**144**:185-200.
13. Palermo M, Silvestri S, Gasparini G, Trombetti T. Crescent shaped braces for the seismic design of building structures. *Mater Struct*. 2015;**48**:1485-1502.
14. Halim H, Hsu HL. Steel A-braced frame upgrade performance under various load characteristics. *J Constr Steel Res*. 2020;**175**:106303.
15. Hsiao PC, Hayashi K, Inamasu H, Luo YB, Nakashima M. Development and testing of naturally buckling steel braces. *J Struct Eng*. 2016;**142**(1):04015077.
16. Liu Y, Iwata K, Sanda S, Nishiyama M, Tani M. Development of curved braces partially strengthened by induction heating. *Eng Struct*. 2021;**233**:111754.
17. AISC. *Design Guide 33: Curved Member Design*. American Institute of Steel Construction; 2018.
18. Rajasekaran S, Padmanabhan SJEM. Equations of curved beams. *J Eng Mech*. 1989;**115**(5):1094-1111.
19. Vacharajittiphan P, Trahair NS. Flexural-torsional buckling of curved members. *J Struct Div*. 1975;**101**(6):1223-1238.

20 Ojalvo M, Demuts E, Tokarz F. Out-of-plane buckling of curved members. *J Struct Div*. 1969;**95**(10):2305-2318.
21 Mazzoni S, McKenna F, Scott MH, Fenves GL. OpenSees command language manual. *Pac Earthq Eng Res Cent*. 2006;**264**(1):137-158.
22 King C, Brown D. *Design of Curved Steel*. Steel Construction Institute; 2001.
23 Abaqus G. *Abaqus 6.11*. Dassault Systemes Simulia Corporation; 2011.
24 Inamasu H, de Castro e Sousa A, Güell G, Lignos DG. Anchor-yield exposed column bases for minimizing residual deformations in seismic-resistant steel moment frames. *Earthq Eng Struct Dyn*. 2021;**50**(4):1083-1100.
25 Matsuo S, Kurata M, Saburi K, Akazawa M, Kawamata Y. E-defense shake table test of four-story steel building with exposed column bases part 2 behavior of structural members. *Summaries of Technical Papers of Annual Meeting, Architectural Institute of Japan, Structures-III*; 2021:1159-1160.
26 Weng CC, Pekoz T. Residual stresses in cold-formed steel members. *J Struct Eng*. 1990;**116**(6):1611-1625.
27 Ingvarsson L. *Cold-Forming Residual Stresses Effect on Buckling*. Proc., 3rd Speciality Conf. on Cold-formed Steel Structures, St. Louis. 1975:85-119.

How to cite this article: Lin K, Kurata M, Kawasaki Y, Kitatani Y. Investigation of low-disturbance seismic retrofit method for steel column bases using curved members. *Jpn Archit Rev*. 2024;7:e12429. https://doi.org/10.1002/2475-8876.12429